Plant Physiology and Biochemistry 135 (2019) 224–232

Contents lists available at ScienceDirect

Plant Physiology and Biochemistry

journal homepage: www.elsevier.com/locate/plaphy

Research article

Resource allocation in response to herbivory and gall formation in *Linaria vulgaris*

Ana Sedlarević Zorić[a], Filis Morina[a,b,*], Ivo Toševski[c,d], Tomislav Tosti[e], Jelena Jović[d], Oliver Krstić[d], Sonja Veljović-Jovanović[a]

[a] Institute for Multidisciplinary Research, University of Belgrade, Belgrade, Serbia
[b] Biology Centre of the Czech Academy of Sciences, Institute of Plant Molecular Biology, České Budejovice, Czech Republic
[c] CABI, Delémont, Switzerland
[d] Institute for Plant Protection and Environment, Department of Plant Pests, Zemun, Serbia
[e] University of Belgrade, Faculty of Chemistry, Belgrade, Serbia

ARTICLE INFO

Keywords:
Carbohydrates
Galls
Herbivory
Linaria vulgaris
Rhinusa pilosa
Source-sink interactions
Trehalose 6-phosphate

ABSTRACT

Trehalose and its precursor, trehalose 6-phosphate (T6P), are essential regulators of plant response to abiotic and biotic stress. Here we used the specific host-insect interaction between *Linaria vulgaris* (Plantaginaceae) and stem-galling weevil, *Rhinusa pilosa* (Mecinini, Curculionidae) with the aim to distinguish carbohydrate allocation patterns in response to herbivory, gall formation (G1, 24 h after oviposition), and gall development (G2, 7 days after oviposition) under controlled conditions. The hypothesis is that herbivory and galling induce distinct responses in both leaves and stems, and that shifts in carbon allocations are regulated by signaling sugars. Systemic response to herbivory was accumulation of T6P and maltose. The main feature of G1 in the stems was accumulation of trehalose, accompanied by increased T6P, turanose and glucose content, oppositely to the leaves. In G2, galls had 3-folds higher weight than controls, with further accumulation of fructose, glucose, turanose, and total water-insoluble carbohydrates (TIC), while the sucrose/hexose ratio decreased. Analysis of fast chlorophyll fluorescence kinetic (OJIP) transients in G2 showed a slight decrease in quantum yield of electron transport flux from Q_A to Q_B, and towards photosystem I acceptor side, correlated with the decreased content of photosynthetic pigments and hexoses accumulation. Redistribution of photosynthates, and accumulation of T6P were induced in response to herbivory, indicating its signaling role. The results support the hypothesis that *R. pilosa* can induce plant reprogramming towards the accumulation of beneficial carbohydrates in developing gall by mechanisms which include both T6P and trehalose.

1. Introduction

Interactions between host plants and gall-inducing insects are remarkable examples of structural, physiological, and chemical manipulations of the plant cells resulting in abnormal plant outgrowths – galls (Tooker and De Moraes, 2008; Giron et al., 2016). Gall initiation and development are manifested by the cell hypertrophy and tissue hyperplasia, as well as by changes in the chemical composition (Giron et al., 2016; Oliveira et al., 2016; Carneiro et al., 2017). Galls are mostly initiated in the zones of active cell division (Weis et al., 1988), such as in the apical meristems (Fay et al., 1996; Barnewall, 2011; Barnewall and De Clerck-Floate, 2012).

Recent studies have shown that leaf gall tissue has altered photosynthetic activity compared to the uninfected one, accompanied by accumulation of soluble sugars and changes in starch content (Oliveira et al., 2011; Castro et al., 2012; Carneiro et al., 2014; Huang et al., 2014). However, most of the studies describe leaf or root galls, while reports on biochemical modifications in stem galls in herbs are rare (St John and Shorthouse, 2000; Raman et al., 2006; Marini-Filho and Fernandes, 2012). Additionally, a number of these studies reflects the changes in the composition of nutrients (C, N), while comparative analysis of soluble sugar profile during stem gall development are scarce (e.g. Agarrwal et al. (2014)). Moreover, specific soluble sugars may act as signaling molecules which regulate gene expression thus modulating growth from the cell to the whole plant level (Rolland et al., 2006; Lastdrager et al., 2014). In this respect, the emerging regulatory roles of sucrose, glucose, trehalose and its precursor trehalose 6-phosphate (T6P) have been described recently (Lastdrager et al., 2014; Xiong et al., 2013; Figueroa and Lunn, 2016).

* Corresponding author. Biology Centre of the Czech Academy of Sciences, Institute of Plant Molecular Biology, České Budejovice, Czech Republic.
E-mail addresses: morina@umbr.cas.cz, filis@imsi.rs (F. Morina).

https://doi.org/10.1016/j.plaphy.2018.11.032
Received 7 September 2018; Received in revised form 27 November 2018; Accepted 27 November 2018
Available online 28 November 2018

Three major hypotheses for explaining the adaptive significance of gall induction and evolution of gall morphology are nutrition, enemy, and microenvironment hypotheses (Stone and Schönrogge, 2003). The nutritional hypothesis states that the advantage of galling herbivores is having a high-quality nutrient source with less plant defensive compounds than other feeding modes (Price et al., 1987; Crespi et al., 1997). The microenvironment hypothesis states that galls shield the insect from unfavourable abiotic conditions (excess ultraviolet radiation, temperature changes and desiccation) which are the major problems for larval development (Stone and Schönrogge, 2003; Price et al., 1987; Crespi et al., 1997; Miller et al., 2009). According to the enemy hypothesis, the gall protects the gall-inducer from its predators, parasitoids and pathogens (Stone and Schönrogge, 2003). Gall-inducing insects are mostly inert during the feeding stage (Price et al., 1987); thus, they are entirely dependent on the nutrient sink formed in the host plant tissue.

Rhinusa pilosa (Gyllenhal, 1838) is a highly specific stem-galling weevil associated with yellow toadflax, *Linaria vulgaris* (Toševski et al., 2015). Based on its narrow host range, *R. pilosa* was selected for investigation as a potential agent for the biological control of yellow toadflax in North America (Gassmann et al., 2014). It is overwintering in the adult stage and appears in early spring when adults start to feed on young yellow toadflax shoots and then start to mate. Oviposition takes place in the apical region of the young growing shoots where eggs are deposited inside the stem pith tissue. Gall development is visible already 48 h after oviposition, and its growth is completed after about 10 days. The complete insect development, from egg to adult, is taking place inside the gall. Finally, the adults feed on the remaining gall tissue for two weeks and create an exit hole to leave the gall (Gassmann et al., 2014). In our previous study, we used the specific interaction of *R. pilosa* and *L. vulgaris* to reveal the mechanisms of gall initiation (Sedlarević et al., 2016). In this model system, gall induction has been attributed to female ovipositional fluid (Barnewall and De Clerck-Floate, 2012), and our study indicated the existence of specific signaling phenolic compounds which might be responsible for successful gall initiation.

Here, the relationship between *L. vulgaris* and *R. pilosa* has been used as a model system to answer the following questions: i) are there specific changes in carbohydrate profile induced by insect feeding, gall initiation and/or subsequent gall growth; ii) how are energy demands of the insect developing in the gall secured (manipulation of source-sink interactions by the galler) iii) how is the primary metabolism (chlorophyll fluorescence, photosynthetic performance) affected by gall formation.

2. Materials and methods

2.1. Plant material and experimental conditions

Experiments were performed over three years, in the period 2016–2018. *Linaria vulgaris* plants with young actively growing stems were selected to ensure optimal conditions for gall initiation and formation. The plants were potted individually and separated into three groups: control plants (C), plants for herbivory experiments (H), and plants for oviposition trials (G1 for 24 h, and G2 7 days after oviposition). Each potted plant was caged with a capped, ventilated plastic cylinder (10 × 35 cm), and the soil surface was covered with coarse sand to reduce excessive moisture inside the cylinder and to make the weevils more visible, as previously described in Gassmann et al. (2014). All plants were kept at 21–24 °C with a 16 h/8 h day/night photoperiod, the maximal light intensity at noon was 200 μmol m^{-2} s^{-1} in a stepwise cycle, and humidity was kept at 60% to allow normal gall development. After hibernation, newly emerged adults (females and males) were placed in pairs on 24 plants for feeding and mating. These plants had visible signs of injury due to insect feeding already after one day, and they were used for analysis of herbivory effects. During one week, the insects were daily transferred to new plants to ensure they have enough food supplies and optimal conditions for mating. Subsequently, the 24 copulated females were separated from the males and transferred for oviposition to 24 new plants. These plants were young and actively growing, with the average stem height of 15 cm. The act of oviposition was registered by eye, and the number of oviposition events was subsequently counted and confirmed under a stereomicroscope (Leica MS5, Mannheim, Germany). Time and day of the oviposition event for each plant were recorded.

For biochemical analysis, 20 stem sections were collected from 20 different control (C) or plants affected by herbivory (H) from the same apical region (upper 1/3) of the stem, at the beginning and at the end of the experiment. Out of 20 sections, leaves and stems from each two were pooled together, to obtain ten samples of control leaves and stems (CL and CS for leaves and stems, respectively) and ten samples of plants affected by herbivory (HL and HS for leaves and stems, respectively), that is five for analysis of pigments, and five for carbohydrate analysis. Gall tissue (apical region) for investigating the initiation phase (G1) was collected 12–24 h after oviposition and it was pooled in the same manner as controls (G1L and G1S for leaves and stems, respectively). For investigating the effects of gall development (growing phase, G2), 7 days after oviposition, 12 samples from 12 individual plants were collected and gall tissue was separated in halves, one half for pigment and the other half for carbohydrate analysis. All samples were kept at −80 °C for biochemical analysis.

2.2. Analysis of fast chlorophyll fluorescence kinetic transients

Direct fast imaging of chlorophyll fluorescence was performed using a macroscopic fluorescence imaging system (FluorCam, closed version, Photon Systems Instruments, Brno, Czech Republic), equipped with a newly developed camera, software version and a measuring protocol that allowed direct measurement of fast fluorescence induction (OJIP), as described in more detail in a publication of this new system (Küpper et al., 2018).

For these experiments, we used 12 control plants and 12 plants with developed galls (growing phase, G2). Leaves were placed in a measuring chamber, ventilated by a stream of water-saturated air at 24 °C, and gently pressed to the glass window by a moist cotton pad fixed with a nylon mesh as described in detail by Küpper et al. (2007). Stems and galls were measured without the chamber, after cutting the plant at the base and wrapping the lower part of the stems in a wet cotton pad. The obtained OJIP curves of dark-adapted samples were normalised by their F_p (equivalent to F_m as saturating irradiance was used) values after background subtraction. Excitation light was supplied by two light panels with blue actinic light (LEDs with 460 nm peak) and supersaturating flashes of 4000 μmol m^{-2} s^{-1}, while another two panels supplied measuring flashes with optimized control electronics for fast kinetics and synchronization with the ultrafast camera. Measurements were conducted using a custom-made protocol according to Küpper et al. (2018). Images were taken through a band-pass filter (684 nm) every 250 μs in the fast beginning of the kinetics, and towards the slower parts the frame rate was gradually reduced to save memory space in the camera. Analysis was done usingthe FluorCam software and a description of the used OJIP-test parameters used in the study, according to Stirbet and Govindjee (2011), is given in Table 1.

2.3. Extraction and analyses of photosynthetic pigments

Frozen leaf and stem samples were extracted in 80% acetone (1:10 w/v) and centrifuged at 10 000 *g* at room temperature, and then the pellets were re-extracted. Supernatants were pooled together, diluted in 80% acetone, and the absorbance was measured at 663 nm, 645 nm and 470 nm. Concentrations of chlorophylls *a* and *b* (Chl *a* and Chl *b*) and carotenoids (Car) were determined spectrophotometrically (Shimadzu UV-2501 PC, Kyoto, Japan) following the equations proposed by

Table 1
Calculations and definitions of JIP parameters according to Stirbet and Govindjee (2011).

$\varphi_{Po} = J_o^{TR}/J^{ABS} = 1- F_o/F_m$	Maximum quantum yield of primary PSII photochemistry
$\varphi_{ET2o} = J_o^{ET2}/J^{ABS} = 1- F_j/F_m$	Quantum yield of the electron transport flux from Q_A to Q_B
$\varphi_{RE1o} = J_o^{RE1}/J^{ABS} = 1- F_i/F_m$	Quantum yield of the electron transport flux until the PSI electron acceptors
$\psi_{ET2o} = J_o^{ET2}/ J_o^{TR} = 1- V_j$	Efficiency/probability with which a PSII trapped electron is transferred from Q_A to Q_B
$\psi_{RE1o} = J_o^{RE1}/ J_o^{TR} = 1- V_i$	Efficiency/probability with which a PSII trapped electron is transferred until PSI acceptors
$\delta_{RE1o} = J_o^{RE1}/ J_o^{ET2} = (1- V_i)/(1- V_j)$	Efficiency/probability with which an electron from Q_B is transferred until PSI acceptors

Lichtenthaler and Wellburn (1983) and the values expressed in μg pigment per g of fresh weight (FW).

2.4. Extraction and analysis of carbohydrates

For soluble sugar analysis, frozen tissues were homogenized in liquid nitrogen and extracted in ultrapure water (1/6, w/v) for 30 min in an ultrasonic bath at 25 °C. Following centrifugation at 10 000 *g* for 10 min at 4 °C, the residues were re-extracted under the same conditions and the supernatants were pooled before analysis similarly as described in Vidović et al. (2015). Standard solutions of glucose, fructose and sucrose were prepared in Ultrapure TKA water at a concentration of 1000 ng ml^{-1}, whereas standard solutions of the other analyzed sugars were prepared at a concentration of 100 ng ml^{-1}. Trehalose 6-phosphate dipotassium salt was purchased from Sigma and prepared at the concentration of 100 ng ml^{-1}. The quality control mixture used for monitoring instrument performance was prepared by diluting standards to concentrations in the range 0.9–100 ng ml^{-1} (depending on the concentration in the samples). Chromatographic separations were performed using a DIONEX ICS 3000 DP liquid chromatography system (Dionex, Sunnyvale, CA, USA) equipped with a quaternary gradient pump (Dionex, Sunnyvale, CA, USA). The carbohydrates were separated on a CarboPac®PA100 pellicular anion-exchange column (4–250 mm) (Dionex, Sunnyvale, CA, USA) at 30 °C. The mobile phase consisted of the following linear gradients (flow rate, 0.7 ml min^{-1}): 0–5 min,15% A, 85% C; 5.0–5.1 min,15% A, 2% B, 83% C; 5.1–12.0 min, 15% A, 2% B, 83% C; 12.1 min, 15% A, 4% B, 81% C; 12.1–20.0 min 15%A, 4% B, 81% C; 20.0–20.1 min 20% A, 20% B 60% C; 20.1–30.0 min 20% A, 20% B 60% C; where A was 600 mM sodium hydroxide, B was 500 mM sodium acetate and C was ultrapure water. Before the analyses, the system was preconditioned with 15% A and 85% C for 15 min. Each sample (25 ml) was injected with an ICS AS-DV 50 Autosampler (Dionex, Sunnyvale, CA, USA). The electrochemical detector consisted of gold as the working and Ag/AgCl as the reference electrode.

For the total water-insoluble carbohydrates (TIC) and starch determination, the pellets from soluble sugar extraction were washed in 80% ethanol at 80 °C, centrifuged, rewashed four times under the same conditions and dried at 40 °C. For starch analysis, the pellet was extracted in water and perchloric acid (1:1 v/v) for 20 min on ice, centrifuged, and re-extracted under the same conditions (modified protocol according to Hansen and Møller (1975)). The combined supernatants were used for starch determination by anthrone method (Sadasivam and Manickam (1992)): 50 μl of the sample was mixed with 50 μl water and 400 μl of anthrone (40 mg of anthrone in 20 ml of H_2SO_4), and the mix was shaken and heated for 8 min at 100 °C. The reaction was stopped by immersion in ice. The starch content was obtained by comparing the absorbance of the sample at 625 nm using glucose as a standard. For TIC analysis, the samples were extracted in 2.5 N HCl at 90 °C for three hours, according to Hedge and Hofreiter (1962) and Sadasivam and Manickam (1992). Following centrifugation, acid neutralization was performed using sodium carbonate. Total water-insoluble carbohydrate (TIC) content was determined by anthrone method (Sadasivam and Manickam (1992)):10 μl of samples were mixed with 90 μl water and 400 μl of anthrone (40 mg of anthrone in 20 ml of H_2SO_4), and the mix was shaken and heated for 8 min at 100 °C. The reaction was stopped by immersion in ice for 5 min. The carbohydrate content was obtained by comparing the absorbance of the sample at 625 nm against a standard curve of glucose (0.1–1 mg ml^{-1}).

2.5. Statistical analysis

The significant effects of herbivory, gall initiation and development on carbohydrates, chlorophyll fluorescence parameters and photosynthetic pigments, were tested with the Mann-Whitney *U* test. Tukey's post hoc test was used to test for significant differences in the contents of individual carbohydrates, starch and TIC among different sample groups. Mann–Whitney *U* test and Tukey's post hoc test were conducted with IBM SPSS statistics software (Version 20.0, SPSS Inc., Chicago, IL, USA). Significance threshold value was set at 0.05.

3. Results

3.1. Gall induction

In this experiment, 100 *L. vulgaris* plants were submitted for gall induction using 24 mated *R. pilosa* females. During the three-week period, 87 galls were successfully initiated. The galled plants were subsequently collected for analysis following the time scale of oviposition as described in M&M. Average fresh weights of upper 1/3 of control stems (relative to oviposition localization) were 0.12 ± 0.01 g. As expected, after 24 h (G1) there was no significant increase in the stem weight, while 7 days after oviposition (G2) gall tissue increased to 0.35 ± 0.06g_{FW}.

3.2. Soluble sugar analysis

The content of total soluble carbohydrates in control stems (CS) was 4.4 ± 0.4 mg g_{FW}^{-1}, in the stems after herbivory (HS) 4.5 ± 0.7 mg g_{FW}^{-1}, while it gradually increased from 5.5 ± 0.6 mg g_{FW}^{-1} in the gall initiation phase (GS1) to 7.0 ± 0.8 mg g_{FW}^{-1} in the seven days-old galls (GS2). In control leaves (CL) the soluble carbohydrates content was about 6.0 ± 1.1 mg g_{FW}^{-1}, in the leaves of plants after herbivory (HL) it was 5.2 ± 0.2 mg g_{FW}^{-1}, while both in GL1 and GL2 leaves the content was decreased (3.9 ± 0.1 mg g_{FW}^{-1} and 4.7 ± 0.1 mg g_{FW}^{-1}, respectively). The main carbohydrates detected were monosaccharides: arabinose, fructose, galactose, glucose, mannose, rhamnose, and xylose; disaccharides: maltose, sucrose, trehalose and its intermediary trehalose-6-phosphate, and turanose; trisaccharide raffinose, and sugar alcohols: galactitol, mannitol and sorbitol (Fig. 1). The content of carbohydrates in both CS and CL at the beginning and at the end of the experiment was not significantly changed (data not shown).

In the stems, insect feeding (HS) induced a significant increase in the content of trehalose 6-phosphate (T6P), and maltose, accompanied by an elevated content of galactose ($p < 0.01$) compared to CS, while the content of galactitol decreased (Fig. 1).

In initiating gall (G1S), the most striking change in the soluble carbohydrates composition was about 14-fold increased accumulation of trehalose, accompanied by significant transient accumulation of mannitol, raffinose and rhamnose compared to CS, HS and GS2 stems. In the same time, sorbitol content decreased, while sucrose level was slightly higher compared to CS (Fig. 1). The accumulation of glucose and turanose was correlated with gall development, reaching the

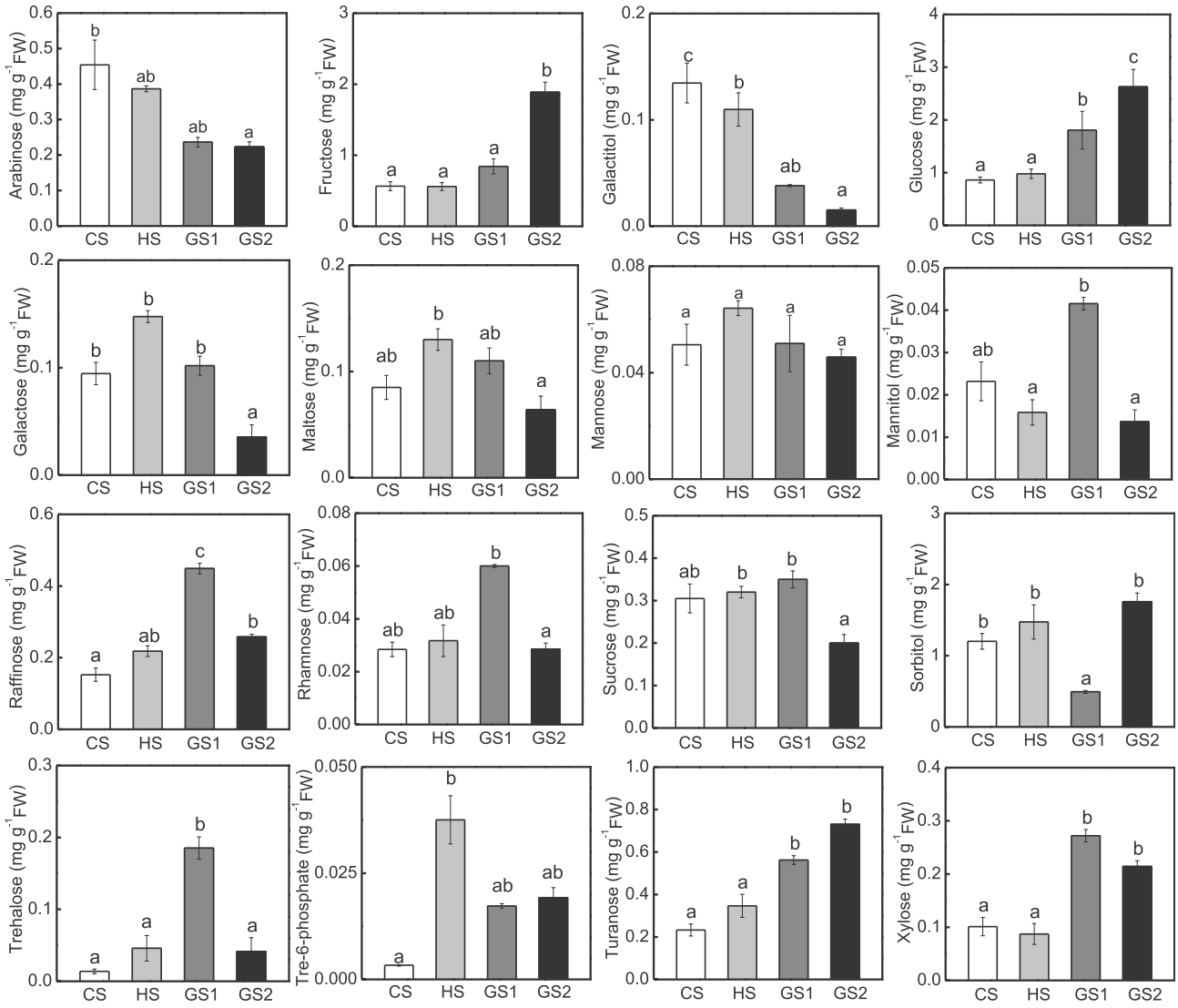

Fig. 1. The content of soluble carbohydrates in *L. vulgaris* control stems (CS), stems after insect feeding (HS), in initiating gall (GS1, less than 24 h) and growing gall (GS2, 7 days after oviposition). Values represent the means ± SE (n ≥ 8). Different letters denote statistically significant differences between the treatments according to Tukey's post-hoc test.

highest values in GS2. Moreover, fructose content in GS2 galls increased significantly compared to both CS and GS1, while xylose remained at the higher level than in CS. Galactitol and galactose contents decreased in developing gall, as well as sucrose. In both GS1 and GS2, the level of T6P was significantly higher compared to CS ($p < 0.01$), although lower than in HS. In comparison to GS1, in GS2 the contents of trehalose, sucrose, mannitol and rhamnose decreased significantly. The content of arabinose significantly decreased only in the developing gall, while mannose was not significantly affected by herbivory or gall development.

In the leaves of plants which were exposed to herbivory (HL), the level of T6P was the highest, similarly as in HS ($p < 0.05$ compared to CL). Further, an increase in arabinose, maltose, mannose, mannitol and rhamnose levels was observed along with a decrease in fructose, galactitol and raffinose compared to CL (Fig. 2), while sucrose content slightly increased. Contrary to the stem galls, the content of T6P was significantly lower in the leaves of plants with initiating and developing galls (GL1 and GL2) than in CL ($p < 0.05$ and $p < 0.01$, respectively). In the leaves of plants with initiating galls (GL1), a transient increase of maltose, mannitol, rhamnose and xylose was observed, while contents of fructose, galactose, galactitol, raffinose, sorbitol, trehalose and turanose declined. Sucrose content remained at the similar level as in HL. In both GL1 and GL2, the content of glucose slightly decreased, while sucrose levels slightly increased. Further, in the leaves of plants with developing gall (GL2) the levels of galactitol, fructose and turanose increased compared to GS1, while sorbitol and xylose remained at the similar level.

3.3. The content of starch and total water-insoluble carbohydrates

Starch content in control stems (CS) contributed about 80% to total water-insoluble sugars (TIC), while in galled stems (GS2) and in the stems which were exposed to herbivory this ratio decreased to about 45–50% (Fig. 3). Moreover, starch content significantly decreased after herbivory (HS) compared to CS, while in the galls no difference in starch content was detected. On the other hand, the content of TIC

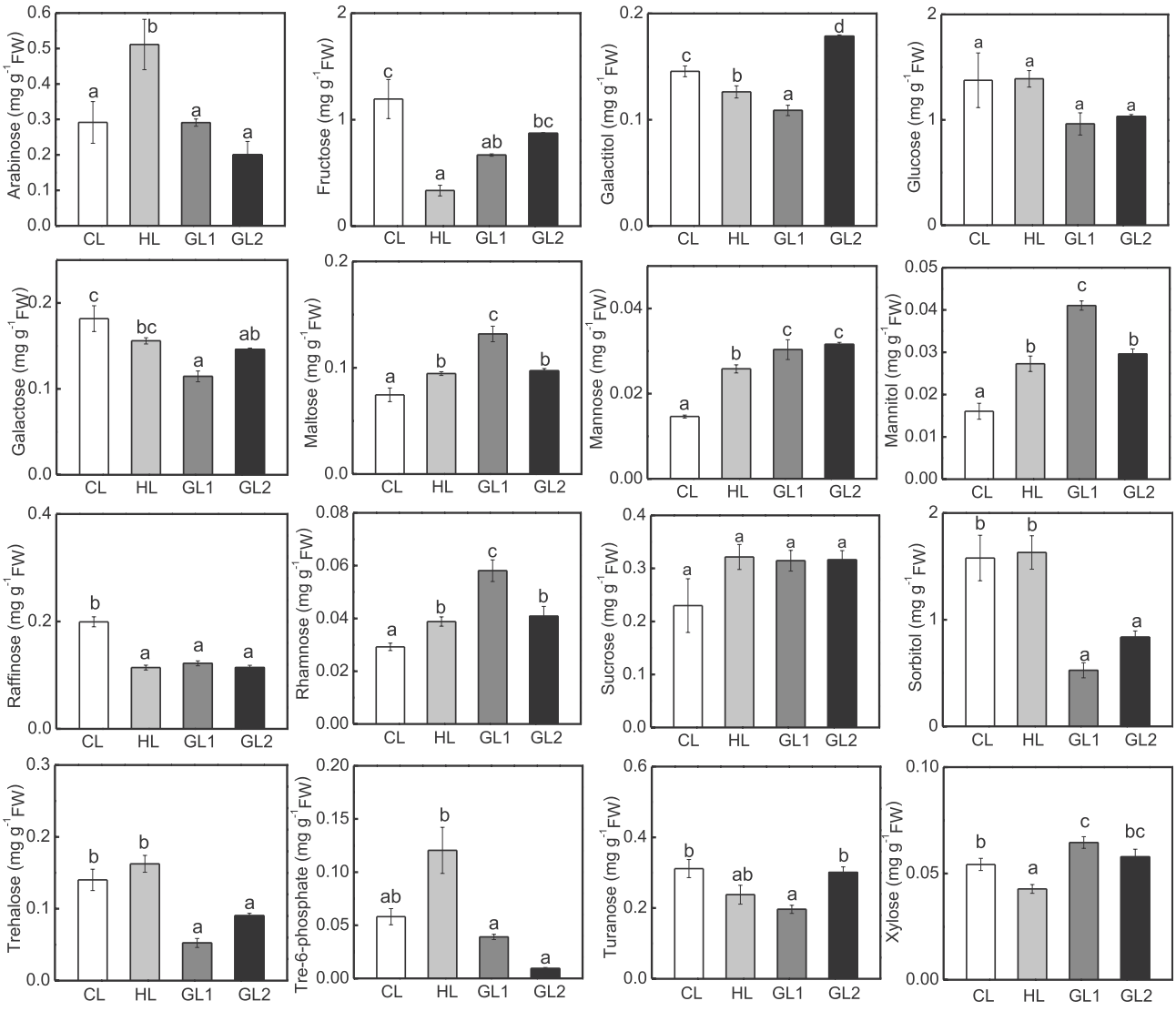

Fig. 2. The content of soluble carbohydrates in *L. vulgaris* control leaves (CL), leaves of plants after insect feeding (HL), and leaves of plants with initiating gall (GL1, less than 24 h) and growing gall (GL2, 7 days after oviposition). Values represent the means ± SE (n ≥ 8). Different letters denote statistically significant differences between the treatments according to Tukey's post-hoc test.

gradually increased with gall development by 1.5- and 1.7-fold compared to control stems ($p < 0.05$ for the significant difference between CS and GS2). In the leaves, there was no significant change in starch or TIC content due to feeding or gall development, and starch contributed about 45–50% to TIC (Fig. 3).

3.4. Analysis of OJIP chlorophyll fluorescence kinetic transients

The fast chlorophyll fluorescence is commonly used as a sensitive tool for detection of changes in photosynthetic electron flow and in the efficiency of photochemistry. The OJIP measurements showed no differences in the leaves regarding the gall development compared to

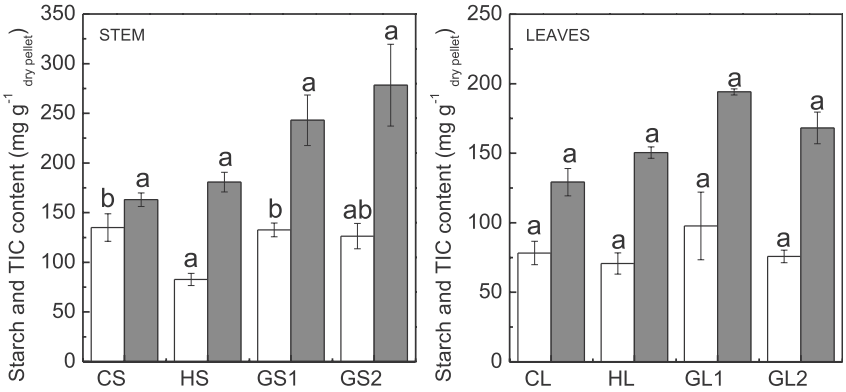

Fig. 3. Content of starch (white bars) and total insoluble carbohydrates (TIC, grey bars) in *L. vulgaris* stems (S) and leaves (L) of control plants (CS, CL), plants after insect feeding (HS, HL), in plants with initiating gall (GS1,GL1, less than 24 h) and in plants with developing gall (GS2, GL2, 7 days after oviposition). Values represent the means ± SE (n ≥ 8). Different letters denote statistically significant differences between the treatments according to Tukey's post-hoc test.

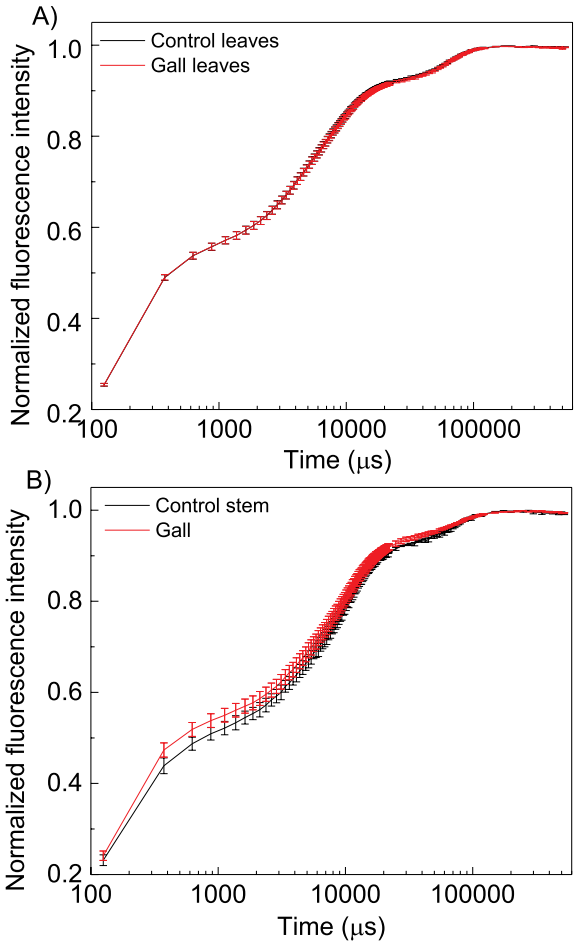

Fig. 4. Kinetic representation of the OJIP transients in A) control *L. vulgaris* leaves and leaves on plants with developing gall, and B) control stems and stem galls seven days after oviposition. Values present average ± SE; n = 12.

Table 2
JIP-test parameters of leaves and stems of control *Linaria vulgaris* plants and leaves and galls seven days after oviposition (G2), numbers represent average ± SE; n = 12; *p < 005, **p < 001,***p < 0001.

	Control leaves	Gall leaves	Control stem	Gall stem
φ_{Po}	0.74 ± 0.02	0.73 ± 0.02	0.77 ± 0.01	0.76 ± 0.04
ψ_{ET2o}	0.57 ± 0.03	0.56 ± 0.04	0.60 ± 0.01	0.58 ± 0.01*
ψ_{RE1o}	0.19 ± 0.03	0.18 ± 0.02	0.17 ± 0.01	0.14 ± 0.01***
δ_{RE1o}	0.34 ± 0.05	0.32 ± 0.04	0.28 ± 0.02	0.24 ± 0.02***
φ_{ET2o}	0.42 ± 0.03	0.41 ± 0.04	0.47 ± 0.01	0.44 ± 0.03*
φ_{RE1o}	0.14 ± 0.02	0.13 ± 0.01	0.13 ± 0.01	0.10 ± 0.01***

Calculations of these parameters are given in Table 1, according to Stirbet and Govindjee (2011).

control plants (Fig. 4A). In contrast, in the seven days old galls, increased Chl fluorescence at $F_{300\mu s}$, F_j and F_i, indicated changes in primary photochemical reactions and electron transport (Fig. 4B).

Although φ_{Po} was not significantly affected, a decrease in quantum yield of electron transport flux from Q_A to Q_B was reduced, as well as further electron transport flux to PSI acceptors indicative by decreased φ_{ET20} and φ_{R10} (Table 2).

3.5. The content of photosynthetic pigments

The contents of Chl *a* and Chl *b* significantly decreased in developing gall, GS2 (2.7 and 2-fold, respectively) compared to control stems, and a lower Chl *a*/*b* ratio was observed (Table 3). Similarly, the

Table 3
Chlorophyll *a* and *b* (μg g_{FW}^{-1}), and their ratio, and carotenoid (Car, μg g_{FW}^{-1}) content in *L. vulgaris* control leaves (CL) and stems (CS) and in leaves and stems of plants with seven days old galls (GL2 and GS2). Values represent the means ± SE (n ≥ 8) *p < 005, **p < 001 and ***p < 0001 indicate the statistically significant difference between control tissues to respective gall tissues.

	Chl *a*	Chl *b*	Chl *a* + *b*	Chl *a*/*b*	Car
CL	1418 ± 200	496 ± 68	1914 ± 265	2.9 ± 0.1	254 ± 22
GL2	1190 ± 403	520 ± 225	1518 ± 734	2.3 ± 0.6	202 ± 16
CS	179 ± 14	47 ± 5	226 ± 18	4.1 ± 0.6	49 ± 4
GS2	62 ± 3***	24 ± 2**	86 ± 5***	2.9 ± 0.8*	28 ± 5*

content of total carotenoids (Car) decreased in the developing gall tissue. However, Car/Chl ratio increased from 0.38 in control stems to about 0.57 in gall tissue. In the leaves of plants with developing gall (GL2), a 2.3-fold decrease of carotenoid content compared to controls was observed, while Chl *a* and Chl *b* were not changed (Table 3). Over the course of the experiment (7 days) the level of photosynthetic pigments was not altered in control stems or leaves (data not shown).

4. Discussion

4.1. Possible roles of trehalose, T6P and hexoses on gall initiation and development

The L. *vulgaris* - *R. pilosa* system presented here allows comparisons of carbohydrate profiles in the time course, during gall initiation and growth, as well as distinguishing the effect of herbivory using plants without galls after *R.pilosa* feeding. Gall initiation provoked immediate, transient accumulation of trehalose in the stems, accompanied by about 5-fold increased content of its intermediate, T6P (Fig. 1). In insects, trehalose is the primary sugar in the haemolymph (Tang et al., 2018); however, to our knowledge, there are no reports on its content in ovipositional fluid. Analysis of *R. pilosa* cecidogen indicated that trehalose was the main sugar component; nevertheless, its concentration was very low (data not shown). Therefore, considering the 14-fold increase in trehalose stem content after oviposition, its accumulation is probably induced by effectors which trigger gall initiation. Such increase in trehalose content during gall initiation might act as an initial signal for cell differentiation and carbon re-allocation. Trehalose is among the crucial virulence factors for *Pseudomonas aeruginosa* in plants (Djonović et al., 2013), while it is also involved in early regulation of metabolic processes in beneficial plant-microbe interactions (reviewed by Figueroa & Lunn, 2016). Additionally, trehalose was crucial for initial rice infection by *Magnaporthe grisea*, while its subsequent degradation allowed pathogen development (Foster et al., 2003). In this study, trehalose content decreased in developing gall after seven days (Fig. 1).

On the other hand, trehalose may induce plant defense responses (Morkunas and Ratajczak, 2014), which could explain the transient increase in the initiating gall, prior to expected transcriptional re-programming by yet unknown effectors from *R. pilosa*. It has been reported that pathogenic bacteria *Xanthomonas citri* which induces citrus canker, synthesize trehalose to modify host plant metabolism to their advantage, while in the same time plants perceive trehalose as a sign of pathogen attack (Piazza et al., 2015).

Besides trehalose and T6P, accumulation of hexoses (glucose, xylose, rhamnose, and raffinose and turanose) was observed upon gall initiation in *L. vulgaris* stem (G1S), without significant changes in the starch content and with the slight accumulation of sucrose (Figs. 1 and 3). Trehalose, T6P and sucrose are essential signaling metabolites which regulate specific responses to environmental signals such as diurnal changes and biotic and abiotic stress (Rolland et al., 2006; Griffiths et al., 2016). Sucrose is the primary photosynthetic product and transport sugar in plants. Majority of sucrose produced in

mesophyll cells is released to the phloem and distributed to the sink tissues where it is cleaved by different invertases to yield monomer hexoses, glucose and fructose (Figueroa and Lunn, 2016; Granot et al., 2013a, 2013b). Trehalose 6-phosphate (T6P) levels are closely related to sucrose concentration in plants (Lunn et al., 2006). T6P has been recently designated as the central signaling molecule that modulates metabolic and developmental processes, and stress responses in plants including source-sink carbon partitioning (Figueroa and Lunn, 2016; Lunn et al., 2014). T6P plays a central role in regulating carbohydrate metabolism, and the role of T6P in orchestrating cell cycle activity and cell wall biosynthesis with cellular metabolism during embryo development has also been implicated (Ponnu et al., 2011). It was shown that T6P inhibits the sucrose non-fermenting 1-related protein kinase1 (SnRK1) complex in Arabidopsis (Zhang et al., 2009). SnRK1 acts as a metabolite sensor to continually adapt the metabolism to the supply and demand of energy (Wurzinger et al., 2018). Moreover, the changes in hexose levels or sucrose: hexose ratio may trigger hexose signaling pathways mediated by hexokinases, target of rapamycin (TOR) and other transcription factors (Xiong et al., 2013; Figueroa and Lunn, 2016; Yadav et al., 2014). Concerning these hypotheses, in our model system, the ratio of sucrose: hexoses decreased from 0.21 in control stems to 0.13 and 0.04 in the initiating (GS1) and developing gall (GS2), respectively.

Glucose accumulation in GS1 and GS2 could have been associated with early organ growth and increased mitotic activity as observed in developing cotyledons (Rolland et al., 2006; Horacio and Martinez-Noel, 2013). The interplay between glucose and phytohormones (auxins, cytokinins, abscisic acid) during plant development has also been shown (Sairanen et al., 2012; Kushwah and Laxmi, 2017). Additionally, turanose accumulation was correlated with gall development (Fig. 1). Stimulating effect of turanose on auxin accumulation has been observed (Gonzali et al., 2005), which may be of importance considering the involvement of auxin and cytokinins in cell growth and division (Oliveira et al., 2016).

The decrease of trehalose and sucrose contents was correlated with the increase of sucrose metabolites, glucose and fructose in developing gall (GS2). The activity of invertase, which catalyses sucrose breakdown to glucose and fructose, was detected in the nutritive tissue of young and mature galls (Rehill and Schultz, 2003; Oliveira et al., 2010). Increased accumulation of soluble carbohydrates in leaf galls compared to uninfected leaves has been reported in several plants (Castro et al., 2012; Hartley, 1998; Huang et al., 2015). Additionally, starch as carbon reserve accumulated in root galls (Griesser et al., 2015), and leaf galls (Oliveira et al., 2010), which was not observed in the stem gall in this study. Similarly as in our study, no increase in the starch content was also observed in leaf galls of *Copaifera langsdorffii* and *Litsea acuminata* (Castro et al., 2012; Huang et al., 2015).

Interestingly, in plants with initiating galls, mannitol, rhamnose, sorbitol and xylose contents have similar trends in both leaves and stems (GL2 and GS2), which may be a systemic response to oviposition. Here the antioxidative function of mannitol should be emphasized (Keunen et al., 2013) considering the increased ROS production in the first stages of enhanced tissue proliferation and growth (Mittler, 2017). Furthermore, T6P, fructose and glucose have opposite (decreasing) response to gall initiation in the leaves (GL1) compared to stems (GS1), which may further support re-allocation of hexoses towards the gall tissue.

Galls provide not only nutrition to the developing insect but also a shelter against enemies, e.g. through fortification of the cell wall (Oliveira and Isaias, 2010; Carneiro et al., 2015). Previously, lignin accumulation has been observed in a mature *L. vulgaris* gall (Barnewall, 2011) which is supported by the increased content of structural sugars, TIC (Fig. 3), and xylose in the developing gall detected in this study. In type I cell wall (Dicot species) the main carbohydrates are cellulose and xyloglucans (Carpita, 2011), while lignin, cross-linked with polysaccharides, confers mechanical strength to the cell wall.

On the other hand, the main systemic response to herbivory was the accumulation of T6P in both HS and HL (Figs. 1 and 2), accompanied by the starch breakdown and maltose accumulation in the stems. The ratio of starch to TIC decreased upon insect feeding (Fig. 3) indicating the differential distribution of carbohydrates. Aphids feeding elicited changes in gene expression associated with carbohydrate metabolism and chloroplasts as well as cell wall modifications in Arabidopsis (Appel et al., 2014). Moreover, the expression of four trehalose phosphate synthase genes was up-regulated by *Brevicoryne brassicae* feeding. Our findings indicate T6P signaling function induced by *R.pilosa* herbivory, which supports the previous reports on the role of trehalose phosphate synthase11 in promoting Arabidopsis defense against the phloem-feeding insects (Singh et al., 2011).

Interestingly, increase in galactose was also observed in *L. vulgaris* stems upon herbivory. Galactose has been indicated in herbivore resistance in *Pseudotsuga menziesii* (Zou and Cates, 1994) and negatively affected the growth rate of *Dineura pullior* (Riipi et al., 2005) and *Epirrita autumnata* (Henriksson et al., 2003). The content of both galactose and its reduction product, galactitiol, significantly decreased in the developing galls.

4.2. Effects of gall development on OJIP chlorophyll fluorescence kinetic transients

Analysis of chlorophyll fluorescence kinetic transients showed significant changes in photosystem II (PSII) photochemistry and electron transport (ET) efficiency in developing galls compared to control ones (Fig. 4, Table 2). This was correlated with a decrease in the amount of Chl *a* and Chl *b* as well as carotenoids in the developing galls (Table 3). Similarly, Aldea et al. (2006) showed decreased photosystem II (PSII) efficiency in the leaf galls of several tree species compared to uninfected leaves. Besides, lower maximum quantum efficiencies for PSII and lower content of pigment-protein complexes were observed in gall leaf portions than ungalled ones (Yang et al., 2007; Huang et al., 2011). Decreased contents of chlorophylls and carotenoids have been observed in galls on *Psidium myrtoides* (Carneiro et al., 2014), leaf galls of *Machilus thunbergii* (Huang et al., 2011) and on *Copaifera langsdorffii* (Castro et al., 2012), while net photosynthetic rate decreased in oak galls (Jiang et al., 2018). On the other hand, no effect on photosynthesis rate was observed in *Aspidosperma australe* following gall formation (Oliveira et al., 2011), while even increased photosynthesis rates were observed in phyllodes with clustered wasp-induced galls than in control ones in *Acacia pycnantha* (Dorchin et al., 2006).

Inhibition of photosynthetic performance in *L. vulgaris* galls may be regulated by accumulated hexoses in the same tissue. It is proposed that hexokinases and fructokinases can sense the accumulated sugars, and repress the expression of photosynthetic genes such as Rubisco and Chl *a/b* binding proteins (Granot et al., 2013a, 2013b), which may be related to observed changes in the galls in this study.

Our results on the decreased quantum yield of electron transport flux from Q_A to Q_B and further until PSI acceptors after seven days compared to control *L. vulgaris* stems (Table 3) indicate limited ability for photosynthesis to support intensive tissue expansion in the gall. On the other hand, in the leaves of galled plants, there was no change in photosynthetic performance compared to control ones, which was correlated with unchanged levels of starch and total insoluble carbohydrates. Considering that plant growth is retarded in relation to dramatic increase of gall biomass during development (about 3-fold compared to control stems), we suggest that the allocation of photoassimilates to the gall as a sink tissue is the main supply of energy for enhanced metabolic processes (Castro et al., 2012; Huang et al., 2015).

The low photosynthesis rate in the galls should provide oxygen and consume CO_2 to stabilize the tissue and protect *R. pilosa* from hypoxia and hypercarbia, as suggested by Oliveira et al. (2016) and Carneiro et al. (2017).

The results obtained in this study show that *R. pilosa* can manipulate

plant resource allocation pattern from the moment of oviposition to gall development by mechanisms which involve T6P and trehalose accumulation. Distinct responses concerning carbohydrate profiles were observed upon herbivory and galling in both stems and leaves, while T6P signaling seems to be involved in both plant responses.

5. Conflicts of interest

There is no conflict of interest relating to this article.

CRediT authorship contribution statement

Ana Sedlarević Zorić: Resources, Formal analysis, Data curation, Writing – original draft. **Filis Morina:** Conceptualization, Methodology, Supervision, Writing – review & editing, Data curation, Formal analysis. **Ivo Toševski:** Conceptualization, Methodology, Writing – review & editing. **Tomislav Tosti:** Methodology, Formal analysis. **Jelena Jović:** Methodology, Writing – review & editing. **Oliver Krstić:** Methodology. **Sonja Veljović-Jovanović:** Conceptualization, Writing – review & editing.

Acknowledgements

This work was funded by 'the Ministry of Education, Science and Technological Development of the Republic of Serbia' [grant numbers III43001 and III43010], and KOROLID Grant [CZ.02.1.01/0.0/0.0/15_003/0000336] funded by 'the Ministry of Education, Youth and Sports of the Czech Republic' with co-financing from the EU.

References

Agarrwal, R., Bentur, J.S., Nair, S., 2014. Gas chromatography mass spectrometry based metabolic profiling reveals biomarkers involved in rice-gall midge interactions. J. Integr. Plant Biol. 56, 837–848.

Aldea, M., Hamilton, J.G., Resti, J.P., Zangerl, A.R., Berenbaum, M.R., Frank, T.D., De Lucia, E.H., 2006. Comparison of photosynthetic damage from arthropod herbivory and pathogen infection in understory hardwood saplings. Oecologia 149, 221–232.

Appel, H.M., Fescemyer, H., Ehlting, J., Weston, D., Rehrig, E., Joshi, T., Xu, D., Bohlmann, J., Schultz, J., 2014. Transcriptional responses of *Arabidopsis thaliana* to chewing and sucking insect herbivores. Front. Plant Sci. 5, 565. https://doi.org/10.3389/fpls.2014.00565.

Barnewall, E.C., 2011. Plant-insect Interactions between Yellow Toadflax, *Linaria Vulgaris*, and a Potential Biocontrol Agent, the Gall-forming Weevil, *Rhinusa Pilosa*. MSc thesis. University of Lethbridge, Canada.

Barnewall, E.C., De Clerck-Floate, R.A., 2012. A preliminary histological investigation of gall induction in an unconventional galling system. Arthropod Plant Interact 6, 449–459.

Carneiro, R.G.S., Castro, A.C., Isaias, R.M.S., 2014. Unique histochemical gradients in a photosynthesis-deficient plant gall. South Afr. J. Bot. 92, 97–104.

Carneiro, R.G., Pacheco, P., dos Santos Isaias, R.M., 2015. Could the extended phenotype extend to the cellular and subcellular levels in insect-induced galls? PloS One 10, pe0129331. https://doi.org/10.1371/journal.pone.0129331.

Carneiro, R.G., Isaias, R., Moreira, A.S., Oliveira, D.C., 2017. Reacquisition of new meristematic sites determines the development of a new organ, the cecidomyiidae gall on *Copaifera langsdorffii* desf (fabaceae). Front. Plant Sci. 8, 1622. https://doi.org/10.3389/fpls.2017.01622.

Carpita, N.C., 2011. Update on mechanisms of plant cell wall biosynthesis how plants make cellulose and other (1→ 4)-β-D-glycans. Plant Physiol. 155, 171–184.

Castro, A.C., Oliveira, D.C., Moreira, A.S.F.P., Lemos-Filho, J.P., Isaias, R.M.S., 2012. Source–sink relationship and photosynthesis in the horn-shaped gall and its host plant *Copaifera langsdorffii* Desf. (Fabaceae), S. Afr. J. Bot., Le 83, 121–126.

Crespi, B.J., Carmean, D.A., Chapman, T.W., 1997. Ecology and evolution of galling thrips and their allies. Annu. Rev. Entomol. 42, 51–71.

Djonović, S., Urbach, J.M., Drenkard, E., Bush, J., Feinbaum, R., Ausubel, J.L., Traficante, D., Risech, M., Kocks, C., Fischbach, M.A., Priebe, G.P., 2013. Trehalose biosynthesis promotes *Pseudomonas aeruginosa* pathogenicity in plants. PLoS Pathog. 9, pe1003217. https://doi.org/10.1371/journal.ppat.1003217.

Dorchin, N., Cramer, M.D., Hoffmann, J.H., 2006. Photosynthesis and sink activity of wasp-induced galls in *Acacia pycnantha*. Ecology 87, 1781–1791.

Fay, P.A., Hartnett, D.C., Knapp, A.K., 1996. Plant tolerance of gall-insect attack and gall-insect performance. Ecology 77, 521–534.

Figueroa, C.M., Lunn, J.E., 2016. A tale of two sugars trehalose 6-phosphate and sucrose. Plant Physiol. (Sofia) 172, 7–27.

Foster, A.J., Jenkinson, J.M., Talbot, N.J., 2003. Trehalose synthesis and metabolism are required at different stages of plant infection by *Magnaporthe grisea*. EMBO J. 22, 225–235.

Gassmann, A., De Clerck-Floate, R., Sing, S., Toševski, I., Mitrović, M., Krstić, O., 2014. Biology and host specificity of *Rhinusa pilosa*, a recommended biological control agent of *Linaria vulgaris*. BioControl 59, 473–483.

Giron, D., Huguet, E., Stone, G.N., Body, M., 2016. Insect-induced effects on plants and possible effectors used by galling and leaf-mining insects to manipulate their host-plant. J. Insect Physiol. 84, 70–89.

Gonzali, S., Novi, G., Loreti, E., Paolicchi, F., Poggi, A., Alpi, A., Perata, P., 2005. A turanose-insensitive mutant suggests a role for WOX5 in auxin homeostasis in *Arabidopsis thaliana*. Plant J. 44, 633–645.

Granot, D., David-Schwartz, R., Kelly, G., 2013a. Hexose kinases and their role in sugar-sensing and plant development. Front. Plant Sci. 4, 44. https://doi.org/10.3389/fpls.2013.00044.

Granot, D., Kelly, G., Stein, O., David-Schwartz, R., 2013b. Substantial roles of hexokinase and fructokinase in the effects of sugars on plant physiology and development. J. Exp. Bot. 65, 809–819.

Griesser, M., Lawo, N.C., Crespo-Martinez, S., Schoedl-Hummel, K., Wieczorek, K., Gorecka, M., Liebner, F., Zweckmair, T., Pavese, N.S., Kreil, D., Forneck, A., 2015. Phylloxera (*Daktulosphaira vitifoliae* Fitch) alters the carbohydrate metabolism in root galls to allowing the compatible interaction with grapevine (*Vitis* ssp) roots. Plant Sci. 234, 38–49.

Griffiths, C.A., Paul, M.J., Foyer, C.H., 2016. Metabolite transport and associated sugar signalling systems underpinning source/sink interactions. Biochim. Biophys. Acta 1857, 1715–1725.

Hansen, J., Møller, I.B., 1975. Percolation of starch and soluble carbohydrates from plant tissue for quantitative determination with anthrone. Anal. Biochem. 68, 87–94.

Hartley, S.E., 1998. The chemical composition of plant galls are levels of nutrients and secondary compounds controlled by the gall-former? Oecologia 113, 492–501.

Hedge, J.E., Hofreiter, B.T., 1962. Methods of estimating starch and carbohydrates. Carbohydr. Chem. 17, 163–201.

Henriksson, J., Haukioja, E., Ossipov, V., Ossipova, S., Sillanpää, S., Kapari, L., Pihlaja, K., 2003. Effects of host shading on consumption and growth of the geometrid *Epirrita autumnata* interactive roles of water, primary and secondary compounds. Oikos 103, 3–16.

Horacio, P., Martinez-Noel, G., 2013. Sucrose signaling in plants a world yet to be explored, Plant Signal. Beyond Behav. 8, pe23316. https://doi.org/10.4161/psb.23316.

Huang, M.Y., Lin, K.H., Yang, M.M., Chou, H.M., Yang, C.M., Chang, Y.T., 2011. Chlorophyll fluorescence, spectral properties, and pigment composition of galls on leaves of *Machilus thunbergii*. Int. J. Plant Sci. 173, 323–329.

Huang, M.Y., Huang, W.D., Chou, H.M., Lin, K.H., Chen, C.C., Chen, P.J., Chang, Y.T., Yang, C.M., 2014. Leaf-derived cecidomyiid galls are sinks in *Machilus thunbergii* (Lauraceae) leaves. Physiol. Plantarum 152, 475–485.

Huang, M.Y., Huang, W.D., Chou, H.M., Chen, C.C., Chen, P.J., Chang, Y.T., Yang, C.M., 2015. Structural, biochemical, and physiological characterization of photosynthesis in leaf-derived cup-shaped galls on *Litsea acuminate*. BMC Plant Biol. 15, 1. https://doi.org/10.1186/s12870-015-0446-0.

Jiang, Y., Veromann-Jürgenson, L.L., Ye, J., Niinemets, Ü., 2018. Oak gall wasp infections of Quercus robur leaves lead to profound modifications in foliage photosynthetic and volatile emission characteristics. Plant Cell Environ. 41, 160–175.

Keunen, E.L.S., Peshev, D., Vangronsveld, J., Van Den Ende, W., Cuypers, A., 2013. Plant sugars are crucial players in the oxidative challenge during abiotic stress extending the traditional concept. Plant Cell Environ. 36, 1242–1255.

Küpper, H., Parameswaran, A., Leitenmaier, B., Trtilek, M., Šetlík, I., 2007. Cadmium-induced inhibition of photosynthesis and long-term acclimation to cadmium stress in the hyperaccumulator *Thlaspi caerulescens*. New Phytol. 175, 655–674.

Küpper, H., Benedikty, Z., Morina, F., Andresen, E., Mishra, A.S., Trtílek, M., 2018. Analysis of OJIP chlorophyll fluorescence kinetics & Q_A re-oxidation kinetics by direct fast imaging. Plant Physiol (Accepted).

Kushwah, S., Laxmi, A., 2017. The interaction between glucose and cytokinin signaling in controlling *Arabidopsis thaliana* seedling root growth and development. Plant Signal. Behav. 12, e1312241. https://doi.org/10.1080/15592324.2017.1312241.

Lastdrager, J., Hanson, J., Smeekens, S., 2014. Sugar signals and the control of plant growth and development. J. Exp. Bot. 65, 799–807.

Lichtenthaler, H.K., Wellburn, A.R., 1983. Determinations of total carotenoids and chlorophylls a and b of leaf extracts in different solvents. Biochem. Soc. Trans. 11, 591–592.

Lunn, J.E., Feil, R., Hendriks, J.H., Gibon, Y., Morcuende, R., Osuna, D., Scheible, W.R., Carillo, P., Hajirezaei, M.R., Stitt, M., 2006. Sugar-induced increases in trehalose 6-phosphate are correlated with redox activation of ADP glucose pyrophosphorylase and higher rates of starch synthesis in *Arabidopsis thaliana*. Biochem. J. 397, 139–148.

Lunn, J.E., Delorge, I., Figueroa, C.M., Van Dijck, P., Stitt, M., 2014. Trehalose metabolism in plants. Plant J. 79, 544–567.

Marini-Filho, O.J., Fernandes, G.W., 2012. Stem galls drain nutrients and decrease shoot performance in *Diplusodon orbicularis* (Lythraceae). Arthropod Plant Interact. 6, 121–128.

Miller, D.G., Ivey, C.T., Shedd, J.D., 2009. Support for the microenvironment hypothesis for adaptive value of gall induction in the California gall wasp, *Andricus quercuscalifornicus*. Entomol. Exp. Appl. 132, 126–133.

Mittler, R., 2017. ROS are good. Trends Plant Sci. 22, 11–19.

Morkunas, I., Ratajczak, L., 2014. The role of sugar signaling in plant defense responses against fungal pathogens. Acta Physiol. Plant. 36, 1607–1619.

Oliveira, D.C., Isaias, R.M.S., 2010. Redifferentiation of leaflet tissues during midrib gall development in *Copaifera langsdorffii* (Fabaceae). South Afr. J. Bot. 76, 239–248.

Oliveira, D.C., Magalhães, T.A., Carneiro, R.G.S., Alvim, M.N., Isaias, R.M.S., 2010. Do Cecidomyiidae galls of *Aspidosperma spruceanum* (Apocynaceae) fit the pre-established cytological and histochemical patterns? Protoplasma 242, 81–93.

Oliveira, D.C., dos Santos Isaias, R.M., Moreira, A.S.F.P., Magalhães, T.A., de Lemos-Filho,

J.P., 2011. Is the oxidative stress caused by *Aspidosperma* spp. galls capable of altering leaf photosynthesis? Plant Sci. 180, 489–495.
Oliveira, D.C., Isaias, R.M.S., Fernandes, G.W., Ferreira, B.G., Carneiro, R.G.S., Fuzaro, L., 2016. Manipulation of host plant cells and tissues by gall-inducing insects and adaptive strategies used by different feeding guilds. J. Insect Physiol. 84, 103–113.
Piazza, A., Zimaro, T., Garavaglia, B.S., Ficarra, F.A., Thomas, L., Marondedze, C., Feil, R., Lunn, J.E., Gehring, C., Ottado, J., Gottig, N., 2015. The dual nature of trehalose in citrus canker disease a virulence factor for *Xanthomonas citri* subsp citri and a trigger for plant defence responses. J. Exp. Bot. 66, 2795–2811.
Ponnu, J., Wahl, V., Schmid, M., 2011. Trehalose-6-phosphate connecting plant metabolism and development. Front. Plant Sci. 2, 70. https://doi.org/10.3389/fpls.2011.00070.
Price, P.W., Fernandes, G.W., Waring, G.L., 1987. Adaptive nature of insect galls. Environ. Entomol. 16, 15–24.
Raman, A., Madhavan, S., Florentine, S.K., Dhileepan, K., 2006. Metabolite mobilisation in the stem galls of *Parthenium hysterophorus* induced by *Epiblema strenuana* inferred from the signatures of isotopic carbon and nitrogen and concentrations of total non-structural carbohydrates. Entomol. Exp. Appl. 119, 101–107.
Rehill, B.J., Schultz, J.C., 2003. Enhanced invertase activities in the galls of *Hormaphis hamamelidis*. J. Chem. Ecol. 29, 2703–2720.
Riipi, M., Lempa, K., Haukioja, E., Ossipov, V., Pihlaja, K., 2005. Effects of simulated winter browsing on mountain birch foliar chemistry and on the performance of insect herbivores. Oikos 111, 221–234.
Rolland, F., Baena-Gonzalez, E., Sheen, J., 2006. Sugar sensing and signaling in plants conserved and novel mechanisms. Annu. Rev. Plant Biol. 57, 675–709.
Sadasivam, S., Manickam, A., 1992. Biochemical Methods for Agricultural Sciences. Wiley Eastern Limited, New Delhi.
Sairanen, I., Novák, O., Pěnčík, A., Ikeda, Y., Jones, B., Sandberg, G., Ljung, K., 2012. Soluble carbohydrates regulate auxin biosynthesis via PIF proteins in Arabidopsis. Plant Cell 24, 4907–4916.
Sedlarević, A., Morina, F., Toševski, I., Gašić, U., Natić, M., Jović, J., Krstić, O., Veljović-Jovanović, S., 2016. Comparative analysis of phenolic profiles of ovipositional fluid of *Rhinusa pilosa* (Mecinini, Curculionidae) and its host plant *Linaria vulgaris* (Plantaginaceae). Arthropod Plant Interact. 10, 311–322.
Singh, V., Louis, J., Ayre, B.G., Reese, J.C., Shah, J., 2011. TREHALOSE PHOSPHATE SYNTHASE11-dependent trehalose metabolism promotes *Arabidopsis thaliana* defense against the phloem-feeding insect *Myzus persicae*. Plant J. 67, 94–104.
St John, M.G., Shorthouse, J.D., 2000. Allocation patterns of organic nitrogen and mineral nutrients within stem galls of *Diplolepis spinosa* and *Diplolepis triforma* (Hymenoptera Cynipidae) on wild roses (Rosaceae). Can. Entomol. 132, 635–648.
Stirbet, A., Govindjee, 2011. On the relation between the Kautsky effect (chlorophyll a fluorescence induction) and photosystem II basics and applications of the OJIP fluorescence transient. J. Photochem. Photobiol., B 104, 236–257.
Stone, G.N., Schönrogge, K., 2003. The adaptive significance of insect gall morphology. Trends Ecol. Evol. 18, 512–522.
Tang, B., Wang, S., Wang, S.G., Wang, H.J., Zhang, J.Y., Cui, S.Y., 2018. Invertebrate trehalose-6-phosphate synthase gene genetic architecture, biochemistry, physiological function, and potential applications. Front. Physiol. 9, 30. https://doi.org/10.3389/fphys.2018.00030.
Tooker, J.F., De Moraes, C.M., 2008. Gall insects and indirect plant defenses: a case of active manipulation? Plant Signal. Behav. 3, 503–504.
Toševski, I., Caldara, R., Jović, J., Hernández-Vera, G., Baviera, C., Gassmann, A., Emerson, B.C., 2015. Host-associated genetic divergence and taxonomy in the *Rhinusa pilosa* Gyllenhal species complex: an integrative approach. Syst. Entomol. 40, 268–287.
Vidović, M., Morina, F., Milić, S., Albert, A., Zechmann, B., Tosti, T., Winkler, J.B., Veljovic-Jovanović, S., 2015. Carbon allocation from source to sink leaf tissue in relation to flavonoid biosynthesis in variegated *Pelargonium zonale* under UV-B radiation and high PAR intensity. Plant Physiol. Biochem. 93, 44–55.
Weis, A.E., Walton, R., Crego, C.L., 1988. Reactive plant tissue sites and the population biology of gall makers. Annu. Rev. Entomol. 33, 467–486.
Wurzinger, B., Nukarinen, E., Nägele, T., Weckwerth, W., Teige, M., 2018. The SnRK1 kinase as central mediator of energy signaling between different organelles. Plant Physiol. 176, 1085–1094.
Xiong, Y., McCormack, M., Li, L., Hall, Q., Xiang, C., Sheen, J., 2013. Glucose–TOR signalling reprograms the transcriptome and activates meristems. Nature 496, 181–186.
Yadav, U.P., Ivakov, A., Feil, R., Duan, G.Y., Walther, D., Giavalisco, P., Piques, M., Carillo, P., Hubberten, H.M., Stitt, M., Lunn, J.E., 2014. The sucrose–trehalose 6-phosphate (Tre6P) nexus specificity and mechanisms of sucrose signalling by Tre6P. J. Exp. Bot. 65, 1051–1068.
Yang, C.M., Yang, M.M., Huang, M.Y., Hsu, J.M., Jane, W.N., 2007. Life time deficiency of photosynthetic pigment-protein complexes CP1, A1, AB1, and AB2 in two cecidomyiid galls derived from *Machilus thunbergii* leaves. Photosynthetica 45, 589–593.
Zhang, Y., Primavesi, L.F., Jhurreea, D., Andralojc, P.J., Mitchell, R.A., Powers, S.J., Schluepmann, H., Delatte, T., Wingler, A., Paul, M.J., 2009. Inhibition of SNF1-related protein kinase1 activity and regulation of metabolic pathways by trehalose-6-phosphate. Plant Physiol. 149, 1860–1871.
Zou, J., Cates, R.G., 1994. Role of Douglas fir (*Pseudotsuga menziesii*) carbohydrates in resistance to budworm (*Choristoneura occidentalis*). J. Chem. Ecol. 20 395-40.